Proceedings of the Seventeenth (2007) International Offshore and Polar Engineering Conference
Lisbon, Portugal, July 1-6, 2007

ISBN 978-1-880653-68-5; ISBN 1-880653-68-0(Set); ISSN 1098-6189 (Set)

Computation of the wavemaking resistance of a Harley surface effect ship

Jeffrey C. Harris and Stéphan T. Grilli
Department of Ocean Engineering, University of Rhode Island, Narragansett, RI, USA

ABSTRACT

Still water resistance tests for a 2.3-m model of a Harley surface effect ship (HSC-SES), completed in August 2002, are presented. Few published studies of such a SES exist, and none provide useful measurements of the wetted surface area, which is needed to extrapolate results and predict full-scale HSC-SES performance. Here, estimates of wavemaking drag are made using free-surface elevations measured within the starboard air cushion. Separately, a numerical model, based on a fast-multipole accelerated boundary element method, is used to model fully nonlinear potential flow wave resistance of moving pressure patches, which correspond roughly to the HSC-SES cushions' footprint. The computed wave resistance roughly agrees with measurements taken during the towing tank tests.

KEYWORDS : Wavemaking resistance; towing tank; numerical wave tank; nonlinear boundary element method; ship waves

INTRODUCTION

In recent years there has been broad interest in high speed ships, not only for special purpose military crafts, but also for fast passenger ferries and commercial sealift (McKesson, 1998). In this respect, one of the most promising concepts is the Surface Effect Ship (SES), which features an air cushion located, unlike hovercrafts, within a cavity built in a rigid hull. Reviews of SES designs can be found in Mantle (1980) and Yun and Bliault (1999). This work presents analyses of selected results of resistance tests performed in a towing tank, on a new type of SES design, the Harley SES. Experimental wavemaking drags are compared to those calculated in an idealized numerical model.

Harley SES

The Harley SES design was patented in 1996, by H. Harley, of Harley Shipbuilding Corporation (HSC) of Bartow, Florida. The HSC-SES, as it is referred to in this paper, is a catamaran ship built with rigid hulls (typically made of highly rigid and resistant carbon-reinforced composite material), having two air cavities (i.e., seal-less air cushions), each pressurized from air-flow inlets at the bow (Fig. 1). Each demi-hull consists of a deep-V bow with a step separating it from the air cushion, two thin sidehulls or fins, which contain the air cushion, and an inverted-V transom stern. A lift fan located at the bow forces pressurized air into the air cushions. Propulsion is achieved typically by twin supercavitating propellers at the stern.

Although HSC built and field tested several large scale models or prototypes of its SES design (including 26- and 65-ft prototypes, as well as a 100-ft fast ferry), scale model testing in a more controlled environment has been desirable, to better assess the hullform's performance and further develop and refine it, in order to achieve sufficient efficiency to consider building larger scale prototypes, having sufficient payload capacity and range. These more detailed performance analyses were conducted by Ocean Dynamics Inc., a former collaboration of HSC and Vibtech Inc. of Wickford, Rhode Island. As a result, several design changes were made to the relative dimensions of the hull, particularly with regards to the cushion's aspect ratio. It is currently thought that the optimal spacing between the demi-hulls is equal to their width, with the twin air cushions having a length to beam (L/B) ratio of 6.5 and extending from the SES stern to a point located 65% of the way to the bow (i.e., 65% of the length overall).

Initial scale model studies, conducted in the 1990s, consisted in towing on a lake over forty 2.3 m models built with composite material and using a load cell to measure total drag. No airflow measurements were made, but it was noticed that, unless some dynamic lift was achieved (e.g., using deep-V bows for planning lift), the design efficiency was limited for large displacements. This finding may imply that the draft towards the bow needs to be small enough for the seal-less air cushion to act efficiently. Various towing tank tests were then conducted at this point.

In the next phase, in 2001, 7.9 m (26 ft) and 16.8 m (55 ft)

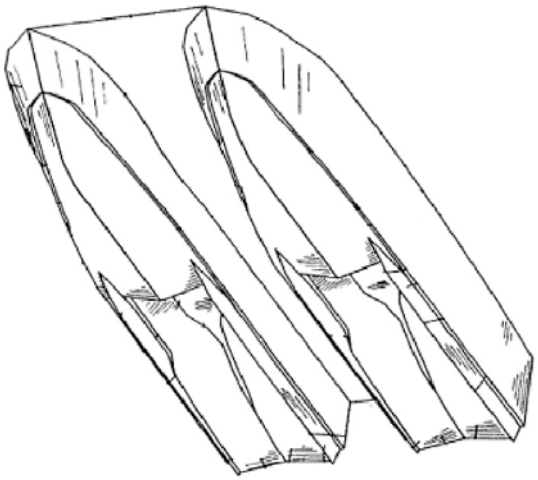

Fig. 1: Harley SES concept hullform, *U.S. Patent*, No. 5570650, 1996.

prototypes were built, as well as small ferries for commercial use. The 7.9 m design had a 3.0 m (10 ft) beam, substantially wider than any later design, and reached 27 m/s (52 kts) with a 86 kW (115 hp) outboard motor and 1724 kg (3800 lb) displacement. The 16.8 m prototype, with 985 kW (1320 hp) propulsion and a 112 kW (150 hp) blower reached 23 m/s (45 kts) at a displacement of 7.98 tons (Latorre et al., 2002). The air cushions covered only 50% of the hulls' length at this point. The latter craft was later extended to 19.8 m (65 ft) and more powerful engines installed, reaching more than 31 m/s (60 kts) during trials. Unfortunately, since none of these vessels have the same relative dimensions (i.e., are geosims), such as the aspect ratio of the air cushions, it is difficult to assimilate and compare this information.

Latorre et al. (2002) studied a microbubble drag reduction (MBDR) method, both during towing tank tests of a 2.3 m HSC-SES model at the NASA/Langley seawater tank, and full-scale trials of the 16.8 m prototype. These tests showed that a drag reduction of 5–15% could be achieved by injecting air bubbles along the sidehulls. This study also has the first estimate of wetted surface area (WSA) of the boat at speed. Unfortunately, scaling laws appropriate to the physics of microbubble drag reduction are not well understood.

Other tests were conducted in 2001 at SSPA in Sweden, in which most notably underwater pictures of the SES were taken at speed (Allenström et al., 2001). Fig. 2, for instance shows the typical wetted areas of the hull, as well as numerous air bubbles that seem to be entrained at the bow; these could reduce the frictional drag of the hull, even without the active production of air bubbles mentioned before. Allenström et al. referred to the design as an Air Lifted Catamaran (ALC), or Skirtless SES, which they are independently developing. Tudem et al., (2004) report the most recently published work on this hullform, conducted by the same research group. Despite their access to data on these hullforms at multiple length scales, their presentation of the physical aspects is still questionable; they appear to estimate the drag for two air cushions as twice the drag of one cushion, rather than considering

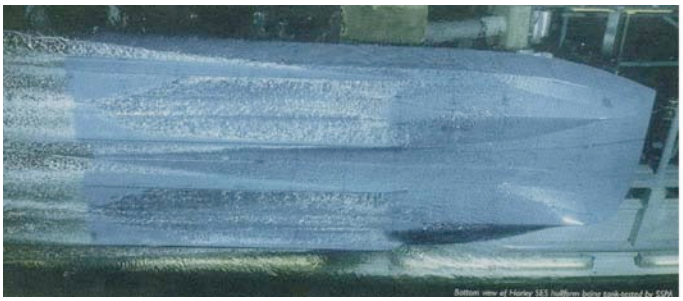

Fig. 2: Underwater view of Harley SES model during testing at SSPA (Allenström et al., 2001).

the interaction between the two (in fact, they comment that their wavemaking drag estimate seems too high).

Unfortunately, the majority of the tests performed on the HSC-SES is poorly documented. Notably the WSA still cannot be clearly estimated, and airflow to the cushions was never precisely measured. The purpose of resistance tests is to determine the power necessary to achieve a desired speed at a given displacement, and part of this power is the power required to produce the airflow to the air cushions. If the airflow is poorly known in either the models or the prototypes, then this could result in either too optimistic or pessimistic estimates of the powering requirements of a full-scale HSC-SES. The present work in part clarifies this issue.

Resistance components

As it is customary in resistance tests, for practical purposes the total still water resistance, D_T, of a ship moving at speed U through water of density ρ can be defined as the sum of different resistance components.

$$D_T = D_F + D_A + D_M + D_R \tag{1}$$

where D_F is frictional drag, D_A is air drag (which may be a large contribution for a fast moving vessel), D_M is momentum drag (specific to SES and other cushion vehicles), and D_R is residual drag (typically wavemaking and form drag). The total resistance must be split up into these separate components because, as we shall see, D_F and D_R depend on different nondimensional numbers, and D_A and D_M may be unrealistic in model testing. Indeed, for convenience, the ship superstructure is not typically reproduced at model scale (and equipment can be added to it), thus strongly affecting the ship aerodynamics, and the SES lift fans inducing the airflow in the cushions can be set outside the model, and hence momentum is differently impaired to the tested model.

For both the SES model and prototype, frictional drag is estimated using a measurement of the wetted surface area (WSA), S_W, as a function of the ITTC-1957 model-ship correlation line that determines the frictional drag coefficient, C_F as a function of Reynolds number **Re** (Newman, 1977),

$$D_F = \frac{1}{2} c_F \rho S_W U^2 \tag{2}$$

$$c_F = \frac{0.075}{(\log_{10}\mathbf{Re} - 2)^2} \quad \text{and} \quad \mathbf{Re} = \frac{U L_{WL}}{\nu} \tag{3}$$

which depends on the waterline length of the ship, L_{WL}, and the viscosity of the water, ν.

For the SES prototype, air drag is ideally estimated from the air drag coefficient, c_A (which could be for instance measured in wind tunnel tests), and main cross-sectional area, S_A, as,

$$D_A = \frac{1}{2} c_A \rho_a S_A \, U^2 \tag{4}$$

where ρ_a is air density. In towing tank tests, however, equipment must often be installed above the model, which perturbs the air flow, and hence, for high speed models, D_A needs to be directly measured. This can be done for instance by towing the model while lifted slightly out of the water, and then measuring the so-called tow force.

Momentum drag is a result of the SES lift fans, located on the prototype, imparting momentum onto the air that is forced into the air cushions, by bringing the speed of that air to the same speed as the ship. For a given fan inlet area of A_i with airflow Q, this is equal to,

$$D_M = Q \, A_i U \tag{5}$$

though in some cases this drag is offset by the fact that there is a similar momentum thrust caused by air leaking from the air cushions. For model testing, however, the fan setup could be entirely different than it would be on an intended ship design (for instance the model fans are typically mounted outside the ship), and D_M too must be measured. This can be done by running the cushion fans and producing the airflow at zero forward speed, while measuring the tow force on the model in still water.

The model residual drag (sum of wavemaking and form drag) is found by subtracting measured or calculated drag components (2),(4), and (5), from the total measured drag D_T. Since it depends on the water surface elevation, i.e., waves generated by the moving ship, D_R is essentially a function of the Froude number **Fr** (Newman, 1977),

$$\mathbf{Fr} = \frac{U}{\sqrt{g L_{WL}}} \tag{6}$$

Accordingly, full-scale ship resistance for a given **Fr** (i.e., tow speed) is found by first Froude scaling the measured D_R as a function of λ^3, where λ is the scale of the geometrically similar model (i.e., a geosim), and adding the frictional, aerodynamic, and momentum drags computed for the full-scale prototype ship. In this computation, the model WSA scales as λ^2, speed scales as $\lambda^{0.5}$.

Cushion airflow

While there have been several theories concerning air leakage from different types of air cushion vehicles (e.g., Mantle, 1980), generally, the steady-state airflow within an air cushion can be represented as a simple axial flow, with an airflow Q entering the inlet of cross-section A_i gradually leaking over a total leakage area A_L (Fig. 3). Bernoulli equation can be used to express the relationship between the cushion pressure, airflow, and leakage area. Ignoring frictional losses (which may not always be a valid assumption), the total air pressure, p, within the cushion is constant and expressed as the sum of a static p_s and a dynamic p_d pressure,

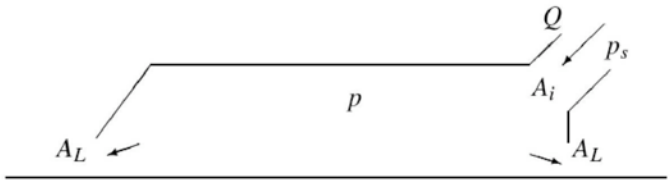

Fig. 3: Sketch of SES cushion flow and leakage.

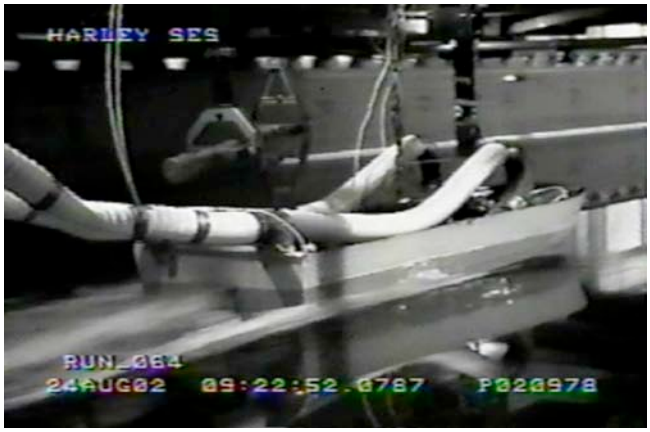

Fig. 4: Towing tank test of of 2.3 m HSC-SES model. Note the tubing provided airflow from the carriage blower.

$$p = p_s + p_d \quad \text{with} \quad p_d = \frac{1}{2}\rho_a v^2 \tag{7}$$

where v is the air velocity at the considered point.

Applying Eq. (7) at the inlet, we find,

$$p = p_{si} + \frac{1}{2}\rho_a \frac{Q^2}{A_i^2} \tag{8}$$

where p_{si} denotes the static pressure at the inlet. Assuming all flow leakage occurs from the cushion to the outside over an area A_L, we find,

$$Q = C_D \, A_L \sqrt{\frac{2p}{\rho_a}} \tag{9}$$

where p is given by Eq. (8) and C_D is a contraction coefficient ($\simeq 0.6$ for a typical SES; Moulijn, 1998).

Note, finally, for steady-state, cushion parameters follow a Froude scaling, although many aspects of air cushion dynamics

Fig. 5: Picture of 2.3 m long HSC-SES model nearly identical to that used in IMD tow tank tests. Cushion inlets are visible as well as the hole for the acoustic range finder.

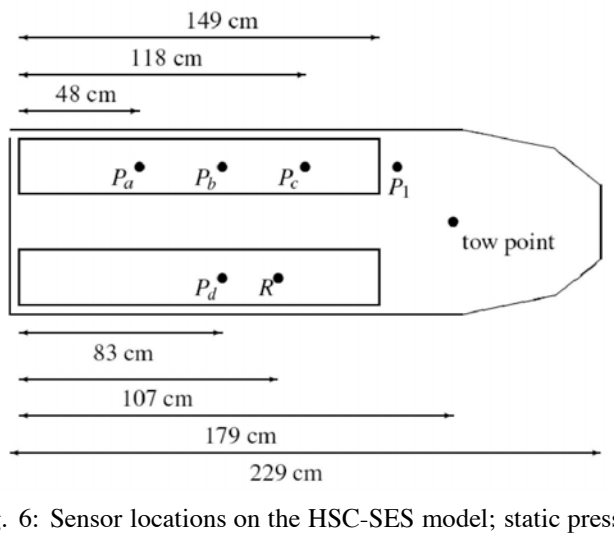

Fig. 6: Sensor locations on the HSC-SES model; static pressure sensors p_a, p_b, p_c, p_d in cushion, and p_1 in the port air inlet. The range finder measured the air gap R in the starboard cushion, 1.07 m from the stern.

do not Froude scale (e.g., cushion stiffness; Moulijn, 1998).

METHODOLOGY

Towing tank setup

A 2.3 m long HSC-SES model was fabricated and used to perform towing tank tests at the Clearwater tank of IMD (St John, Newfoundland), which has a total length of 200 m, a 12 m width, and a 7 m water depth (Fig. 4, 5). An air blower was positioned on the tow carriage, above the model, and provided airflow to the twin model cushion inlets through flexible tubing (Fig. 4). The SES model was free to heave, pitch and roll.

The Clearwater tank is a freshwater tank; while the water temperature was not recorded, it is assumed to be 15 degrees Celsius. The tank carriage can reach a top speed of 9 m/s and maximum tow force for the load cell used in the test was ±250 N. No turbulence inducers were used, but for nearly all tests the Reynolds number was greater than 5×10^6 (the slowest tests at 2 and 4 m/s corresponded to Reynolds numbers of 2.6×10^6 and 5.2×10^6, respectively). While the waterline length (which determines the Reynolds number and thus the frictional drag coefficient) was not measured directly, observations indicated that it is roughly equal to the length of the air cushions, or 1.5 m, 65% of the length overall.

The depth of a towing tank becomes significant (i.e. deep-water assumption becomes invalid) for speeds around and above the critical speed, $\sqrt{gh}$, where h is the water depth, which here is 8.3 m/s. Nondimensionally, the critical speed is reached when the depth Froude number, $F_d = U/\sqrt{gh}$, is 1.0.

Model setup

The 2.3 m long HSC-SES model had a 0.75 m beam and was instrumented with a variety of sensors Fig. 6). Data at all sensors was recorded at a sampling frequency of 50 Hz. Video cameras observing the sidehulls were unfortunately unable to provide useful information about the WSA of the model.

Specifically, pressure sensors were installed, to measure the air pressure within the air cushions and in the air cushion inlets (Fig. 6), by drilling small pressure ports in the air cushions and running small diameter tubing from these ports to the sensors contained separately. The sensors then measured the pressure difference between the air cushion at the specific pressure port and the outside air. Because these were differential sensors, this data was tared using the average recorded pressures when the blower fans were off, and the model was not moving. As seen in other studies performed in the David Taylor Naval Ship R&D Center (Bradley, 1981), pressure sensors installed in such a manner (as opposed to flush-mount pressure transducers) can have static pressure errors on the order of 100 Pa, due to water accumulating in the tubing. This type of error did not permit accurate measurements of average pressures within the cushions for much of the testing. A high frequency acoustic range finder was installed to measure the air gap at one point within the starboard air cushion (Figs. 5, 6), and accelerometers were used to measure the surge and heave accelerations at the tow point (Fig. 6).

Each model air cushion was 1.5 m long and 0.23 m wide (Fig. 7), so the cushion area S_c was 0.68 m^2. The cushion inlets which were connected to the air ducts, were 0.108 m in diameter and placed at a 30^o angle from horizontal (Fig. 5). The cushion height above the keel was 0.18 m. The tunnel area between the twin cushions was approximately 0.23 m across, and 2.5 and 3 cm higher than the keel at the stern and bow, respectively.

The maximum possible leakage cross-sectional areas at the bow and stern were measured approximately as 0.006 m^2 and 0.007 m^2, respectively. This results in a maximum possible leakage area of approximately 0.013 m^2, assuming no air is leaking underneath the keels of the sidehulls.

Numerical simulations

The numerical model developed by Sung and Grilli (2005) was used to independently estimate wavemaking drag and compare it to measurements. This is a fully nonlinear potential flow

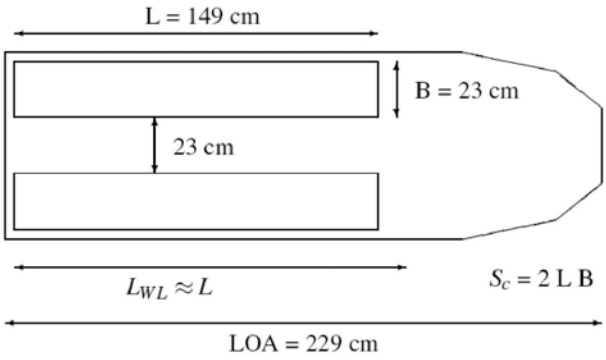

Fig. 7: Schematic of air cushion dimensions for the 2.3 m HSC-SES model. The waterline length, L_{WL}, is slightly greater than the length L of the cushions of surface $S_c = 0.685$ m^2.

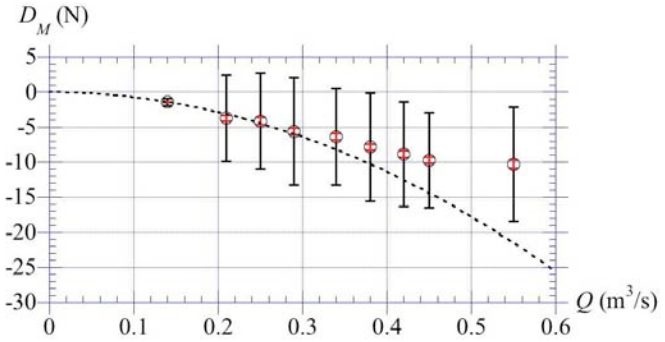

Fig. 8: Measured momentum drag (for $W = 289$ N): mean (o) ± standard deviation (—), and 95% confidence interval for the mean (red —); compared to theoretical Eq. (10) (- - -).

model, expressed in a coordinate system moving with the ship. Laplace's equation is solved using a Boundary Element Method (BEM). In the present versions, computations are accelerated by using a Fast Multipole Algorithm (FMA; Fochesato and Dias, 2006). In this paper, we present simulations of waves created by two moving pressure patches, which roughly correspond to the HSC-SES model, i.e., two patches with the same dimensions as the SES air cushions. More detailed comparisons between numerical and experimental results are given by Harris (2007). The model has been under continuing development, testing a variety of free-surface updating schemes.

RESULTS

The model was tested for various airflows in the cushions, corresponding to seven different blower/fan speeds (i.e., Revolutions Per Minute; RPM), for different model displacements or weight W, and horizontal position of the center of mass l_{cg}.

Momentum drag tests

The static tow force measured during RPM tests, done at zero forward speed ($U = 0$), is a measure of the momentum drag caused by the airflow Q entering the cushions, through inlets of cross-section A_i, and changing speed to come to rest in the cushion. Hence, theoretically,

$$D_M = -\rho_a \frac{Q^2}{A_i} \tag{10}$$

In experiments, vendor's fan curves provide Q as a function of a specified RPM at the blower and the static pressure measured at the inlet (p_1 in Fig. 6; see Harris, 2007 for detail).

Fig. 8, for instance, shows the momentum drag measured as a function of airflow Q, corresponding to various RPMs, for a HSC-SES model of displacement $W = 289$ N. Most of these D_M measurements were quite noisy, due to significant vibrations of the model, except for the lowest airflow (fan speed RPM = 1,200). This is reflected in the figure by the large standard deviation of individual measurements, except for the lowest Q value. The distinguishing feature of this low airflow/fan speed is that the total pressure applied to the air in the cushions was not sufficient to force it out through the sidewalls. For larger RPMs, from the video recordings made within the cushions, waves can be seen moving aft where air leaks out the sides of the cushions in gusts.

Eq. (10) is also plotted in Fig. 8. For moderate airflows less than 0.3 m^3/s, the mean measured and theoretical momentum drags agree well. For higher airflow, the deviation is likely due to excess air being forced forward out of the cushions through the stern. Because it was observed that steady air leakage mostly happened from the bow, and not from the stern, this difference is probably not important for resistance tests, where the trim angle is only on the order of one degree.

Air drag tests

Air drag was measured by raising the model slightly out of the water and measuring the drag force when towed. Fig. 9 shows mean and standard deviation of the measured tow force, as well as 95% confidence intervals for the mean; the latter are quite narrow, implying the measured mean is accurate. The large standard deviation of individual measurements is most likely due to vibrations of the model, which is suspended to the tow carriage. The carriage load cell is designed to measure tow forces in a ±250 N range, with the model hull in the water. Hence, small oscillations of the total resistance would probably be damped; this is not however the case for air drag measurements, which are around 15 N.

The theoretical Eq. (4) is also plotted in Fig. 9, with an effective cross-sectional area, $c_A S_A = 0.30$ m^2, that was estimated based on a least-squares fit to the mean measured data. Thus, as would be expected for a turbulent flow, the mean air drag varies with the square of the tow velocity.

Resistance tests

Total resistance/drag D_T was measured in resistance tests, as a function of model displacement W, blower RPM, and tow speed U. For each test, both cushion and inlet pressures were measured

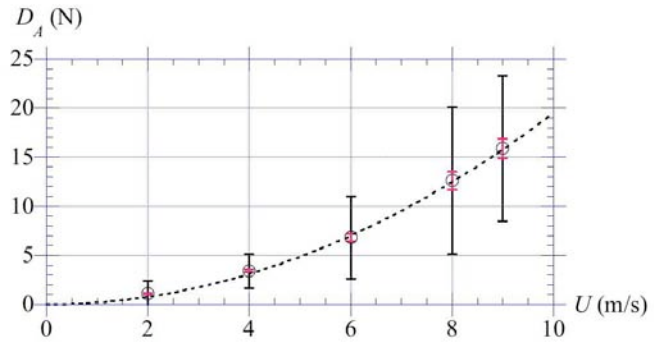

Fig. 9: Measured air drag : mean (o), $\pm$ standard deviation (—), and 95% confidence interval of the mean (red —) compared to theoretical Eq. (4) with $c_A\, S_A = 0.30\ \mathrm{m}^2$.

W (N)	RPM	4 (m/s)	6 (m/s)	8 (m/s)	9 (m/s)
	4140	32.09	43.70	47.33	50.97
445	3000	35.80	49.65	55.40	60.35
	2400	39.83	58.73	69.00	
	4140	20.39	30.32	39.57	
356	3000	24.69	37.56	45.60	
	2400	26.69	43.32	54.78	
	4140	13.67	23.42	33.99	52.16
289	3000	17.26	32.34	40.24	
	2400	19.64	36.43	47.27	

Table 1: Selected corrected hydrodynamic drag measurements $D_T - D_M - D_A$ (N), averaged and tared, as a function of model displacement W (N), blower RPM, and speed U (m/s).

as well as the model trim angle and draft, and range finder data.

Similar to the momentum and air drag tests, the standard deviation of the total drag measurements was found quite large for all tests. This could be due to a number of physical factors, such as instabilities caused by high airflows in the cushions, oscillations within the air ducts, or model porpoising. However, since such a noisy response was never observed in the larger scale HSC-SES prototypes, it is believed it is due to model and test set-up. One early test (with an unrecorded displacement, $U = 1.5$ m/s, and 1800 RPM or $Q = 0.23\ \mathrm{m}^3$/s), was run at speed both with and without the air blower turned on, and indeed showed that vibrations only occurred in the tow force measurement when the blower was on. Thus, it is possible that the air blower itself is causing the tow carriage to vibrate, but we cannot form a definite conclusion with the available data. Since the mean total drag is well repeatable between tests, these vibrations were deemed unimportant.

According to Eq. (1), the mean total drag measurements were corrected for mean measured momentum (i.e., using Eq. (10): -5.57 N, -9.20 N, and -19.9 N, for 2400, 3000, and 4140 RPM tests, respectively) and air drag (Eq. (4) with $c_A S_A = 0.30\ \mathrm{m}^2$). Corrected average results are given in Table 1. As expected, most corrected hydrodynamic drags increase with increasing W and U, and decrease with increasing RPM (i.e., airflow Q). This trend is not strictly found in a few measurements, which could be due to inaccuracies in momentum drag corrections (a noisy measurement, as discussed before), or simply to changes in WSA, in relation to model dynamic draft. Often, the air gap within the cushion, detected by the range finder, decreased with increasing airflow. Though sometimes erratic, the range finder data was corrected to measure the change in water surface height within the cushion, below the range finder (Table 2).

W (N)	RPM	4 (m/s)	6 (m/s)	8 (m/s)	9 (m/s)
	4140	-23.5	- 4.9	0.5	5.0
445	3000	-24.1	-18.3	-8.8	3.1
	2400	-27.1	-15.5	N/A	
	4140	-11.9	-4.7	4.6	
356	3000	-18.2	-10.5	-0.2	
	2400	-21.7	-13.9	-5.7	
	4140	N/A	N/A	6.3	N/A
289	3000	N/A	N/A	N/A	
	2400	N/A	N/A	N/A	

Table 2: Change in free-surface elevation within the air cushion underneath the range finder (mm), for tests in Table 1. Faulty measurements are marked as N/A.

Numerical tests

Three test cases were considered in numerical simulations corresponding to the U =4, 6, and 8 m/s cases at $W = 445$ N displacement. The applied pressure in the modeled twin cushions was defined with a distribution similar to Doctors and Sharma's (1972) (also used in Sung and Grilli, 2005), with falloff parameters $\alpha = 5$ and $\beta = 10$, based on the average pressure needed to support the displacement or $p_o = W/S_c = 649$ N. More details are given by Harris (2007).

Though after a long computation time the test cases became unstable, all achieved a quasi-steady state surface wave elevation with a classic Kelvin wave pattern (Fig. 10), and stable total wave drag values. For a simple pressure patch, wave drag D_W^{num} is the integral of the surface pressure p_o, projected in the direction of motion. Results are given in Table 3.

DISCUSSION

Experimental results

Assuming a constant free surface slope in the cushions, the wavemaking drag part of resistance tests can be expressed as a function of the distance to the surface, ΔR, measured with the range finder (Fig. 11),

$$D_W^{exp} = -W\frac{\Delta R}{x_R} \tag{11}$$

with $x_R \simeq 0.42$ m, the distance between the front of the cushion and the range finder (Fig. 6). Because of increased vibrations for high airflow, only the lowest airflow (RPM = 2,400) and highest displacement ($W = 445$ N) tests are used to determine the wavemaking drag D_W^{exp} with Eq. (11) (Table 3). Unfortunately, the $U = 9$ m/s data did not provide an accurate reading of the wake within the air cushion at this RPM (Table 2). Hence only $U = 4$, 6, and 8 m/s are shown in Table 3.

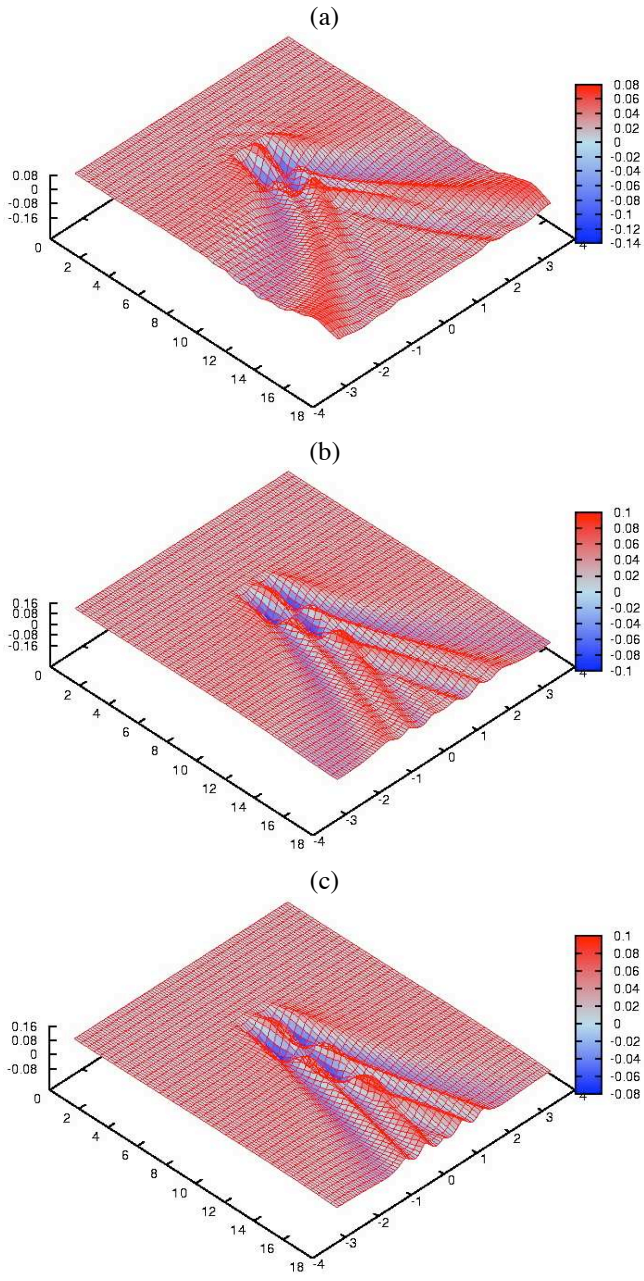

Fig. 10: Computed nondimensional free surface elevations at quasi-steady state, for $W = 445$ N and $U =$ (a) 4, (b) 6, and (c) 8 m/s, established after 300 time steps (corresponding to $t = 18$, 12, and 9 s, respectively).

Assuming all residual drag is due to wavemaking $D_R \simeq D_W$ (which is nearly the case for a shallow draft, high speed, SES),

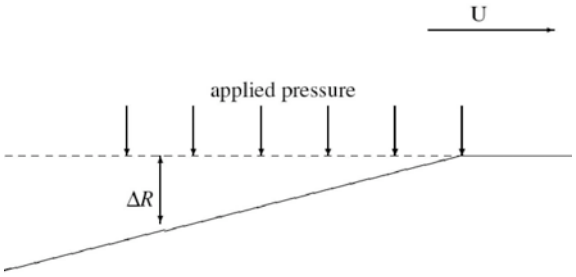

Fig. 11: Schematic of the HSC-SES cushion free-surface at high speed, U; ΔR is the depression measured at the range finder.

U (m/s)	4	6	8
D_W^{exp} (N)	28.7	16.4	9.3
D_W^{num} (N)	18.3	13.4	9.5

Table 3: Estimated wavemaking drag (N), for $W = 445$ N displacement tests, both experimental and numerical.

and calculating the wavemaking resistance with Eq. (11), the model WSA follows from Eqs. (1) and (2) as,

$$S_W = \{D_T - D_M - D_A - D_W\}\{\frac{1}{2}\rho C_F U^2\}^{-1} \qquad (12)$$

Eq. (12) has been used to compute results in Table 4. In order to also handle other displacements (i.e., the 356 and 289 N tests), approximately linear free-surface boundary conditions are assumed. Then free-surface elevation scales linearly with pressure, as does the displacement of the ship, so from Eq. (11), the wavemaking drag scales with the square of the displacement (for a given cushion size).

W (N)	RPM	4 (m/s)	6 (m/s)	8 (m/s)
445	4140	0.65	0.64	0.42
	3000	0.42	0.56	0.40
	2400	0.43	0.63	0.49
356	4140	0.61	0.52	0.38
	3000	0.40	0.46	0.34
	2400	0.34	0.50	0.39
289	4140	0.59	0.47	0.35
	3000	0.36	0.44	0.31
	2400	0.32	0.44	0.34

Table 4: WSA S_W (m^2) estimates for selected tests.

We see that WSA estimates in Table 4 are similar to the cushion area ($S_c = 0.68$ m^2). Thus, the minimization of WSA provided by a SES is mostly negated by being a catamaran.

Comparison of experiments to numerical simulations

The free-surface elevation in the cushion is the most straightforward variable to compare between the numerical and experimental HSC-SES results (Fig. 12). A simple visual comparison

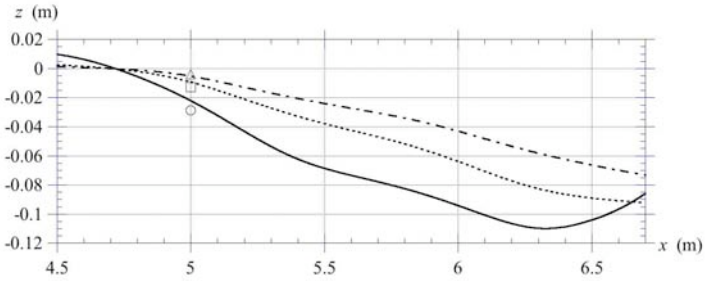

Fig. 12: Nondimensional comparison of computed quasi-steady state free surface cross-sections through one cushion, with the experimentally measured distance at the range finder, for 4 m/s (—), 6 m/s (- - -), and 8 m/s (– – –), as in Fig. 10.

shows that the two are relatively similar at the depth finder location, though in every case the computed free surface is not as depressed as the experimental one. This could be a result of using a mostly constant pressure within the air cushions in the numerical computation, as opposed to the real situation, where the air pressure would be higher at the cushion bow and decrease towards the aft. The main difficulty in improving the simulations would be to determine the appropriate pressure distribution to use.

Unfortunately, it is difficult to infer the experimental free-surface profile from the installed sensors. A more sophisticated approach would be to take the cushion pressure distribution and airflow data to intuit the leakage area, and determine the required free-surface elevation at the stern, but details of the HSC-SES pressure within the cushion are not known to a precision that would allow such an analysis. Thus, in Eq. (11), it is simply assumed that the cushion free surface is a sloping plane; clearly this represents an approximation whose accuracy will be less at low speed, as can be seen in Fig. 12. A consequence of this is, the WSA, calculated from Eq. (12) will also be less accurate at lower speed. To improve on this would require a coupling between an airflow model and the NWT. Therefore, while our current analysis is both simplified and preliminary, we found that a more sophisticated approach does not provide better information at this time due to lack of proper experimental data.

Calculated wave resistances are given in Table 3 for the three cases. Simulations roughly match the experimental results for $U = 6$ and 8 m/s, but provide quite a different answer for $U = 4$ m/s. This could be related to the absence of a hull in the numerical model, which would affect results more at slower speed.

The eventual instability of some numerical simulations was not clearly understood by Sung and Grilli (2005). Further improvement of the numerical model would be important before using this as a design tool.

CONCLUSIONS

Towing tank results of a 2.3 m HSC-SES model were evaluated. Resistance estimates are made at a variety of speeds and displacements. Because the model WSA was not measured, extrapolating resistance measurements to full-scale requires a crude estimate of wavemaking drag. This estimate was made using range finder measurements of the free-surface within the air cushions. Free-surface elevation within the cushion roughly agreed with numerical simulations of two moving pressure patches, corresponding to the HSC-SES cushions setup. While some of the towing tank results remain questionable because of excessive airflow, the overall resistance of the HSC-SES is roughly quantified.

REFERENCES

Allemström, B., and Liljenberg, H., and Tudem, U. (2001) "An airlifted catamaran – hydrodynamical aspects," in *FAST 2001*, Southampton, UK: RINA.

Bradley, C. (1981) "Surface effect ship air cavity pressure gauges," David Taylor Naval Ship R&D Center, Tech. Rep DTNSRDC/CID-81/1.

Butler, E. (1985) "The surface effect ship," *Naval Eng. J.*, **97** 200–260.

Doctors, L. and Sharma, S. (1972) "The wave resistance of an air-cushion vehicle in steady and accelerated motion," *J Ship Res.*, **16**, 248–260.

Fochesato, C. and F. Dias (2006) "A fast method for nonlinear three-dimensional free-surface waves," *Proc. R. Soc.* **A** 2715-2735, doi:10.1098/rspa.2006.1706.

Harris, J.C. (2007) *Understanding and optimizing the Harley surface effect ship,* Master's thesis. Univ. of Rhode Island U.S.A, 130 pps.

Latorre, R., Miller, A. and R. Philips (2002) "Micro-bubble r esistance reduction for high speed craft," *SNAME Transactions,* **110**, 259-277.

Mantle, P.J. (1980) "Air cushion craft development," David Taylor Naval Ship Res. and Dev. Center, 80/012.

McKesson, C.B. (1998) "Hull form and propulsor technology for high speed sealift," *High-Speed Sealift Tech. Wshp.* Center for the Comm. Deployment of Trans. Tech.

Moulijn, J.C. (1998) "Scaling of air cushion dynamics," Delft Univ. of Tech., Report 1151, Project Code 961.

Newman, J., (1977). *Marine Hydrodynamics*, MIT Press Cambridge, MA (9th reprint).

Sung, H., and Grilli, S. (2005) "Numerical modeling of nonlinear surface waves caused by surface effect ships. Dynamics and kinematics," *Proc. 15th Offshore and Polar Engng Conf.* (ISOPE05, Seoul, Korea, 6/05), **3**, 124-131.

Tudem, U. et al. (2004) "Design development of 24 m air supported vessel (ASV) catamaran demonstrator," *High Speed Craft: Design & Operation*, RINA, London, UK.

Yun, L., and Bliault, A. (1999) "Theory and design of air cushion craft," John Wiley and Sons.

ACKNOWLEDGEMENT

This work was supported by Ocean Dynamics Inc., RI, USA. The late John Hopkinson, President of ODI, was the driving force behind the project. The first author's work was partially supported by a National Defense Science and Engineering Graduate fellowship.